

Rapid T_2 Estimation With Phase-Cycled Variable Nutation Steady-State Free Precession

Sean C.L. Deoni,^{1,2} Heidi A. Ward,³ Terry M. Peters,^{1,2,4} and Brian K. Rutt^{1,2,4*}

Variable nutation SSFP (DESPOT2) permits rapid, high-resolution determination of the transverse (T_2) relaxation constant. A limitation of DESPOT2, however, is the presence of T_2 voids due to off-resonance banding artifacts associated with SSFP images. These artifacts typically occur in images acquired with long repetition times (TR) in the presence of B_0 inhomogeneities, or near areas of magnetic susceptibility difference, such that the transverse magnetization experiences a net phase shift during the TR interval. This places constraints on the maximum spatial resolution that can be achieved without artifact. Here, a novel implementation of DESPOT2 is presented incorporating RF phase-cycling which acts to shift the spatial location of the bands, allowing reconstruction of a single, reduced artifact-image. The method is demonstrated in vivo with the acquisition of a 0.34 mm³ isotropic resolution T_2 map of the brain with high precision and accuracy and significantly reduced artifact. Magn Reson Med 52:435–439, 2004. © 2004 Wiley-Liss, Inc.

Key words: T_2 mapping; phase-cycled SSFP; fast imaging; human imaging

We have previously described a novel combined set of T_1 and T_2 mapping techniques based on the acquisition of two or more spoiled gradient recalled echo (SPGR) and fully balanced steady-state free precession (SSFP) images (1). From the multiple SPGR images acquired with constant repetition time (TR) and varied flip angle (α), T_1 can be extracted through an unusual linearization of the SPGR signal equation, first described in Ref. 2. Combining this T_1 information with data from multiple SSFP images also acquired with constant TR and varied α , allows T_2 to be determined through a similar linearization of the SSFP signal equation (1). In addition to introducing these techniques, named DESPOT1 and DESPOT2 for their T_1 and T_2 determination properties, respectively, we have also examined the influence of flip angle choice on the T_1 and T_2 estimate precision and have examined the use of a

weighted least-squares algorithm for determining T_1 and T_2 , introducing an appropriate weighting function that maximizes estimate precision (3).

The primary limitation of the DESPOT2 method is the appearance of voids or artificially low T_2 values in the calculated maps resulting from the well-known off-resonance banding artifact in SSFP images (4). These artifacts present as bands of signal voids and result from any condition that leads to the transverse magnetization incurring a net phase shift during the TR interval, including B_0 inhomogeneities and susceptibility differences, such as those seen near the sinuses and within the structures of the inner ear. These artifacts are bothersome as they prevent ultra-high-resolution (<0.7 mm³ isotropic resolution) T_2 mapping, since such high resolution demands long TR values (typically >6 ms). Minimizing TR is a commonly used and easy approach to reducing the appearance of these artifacts. Unfortunately, this places restrictions on the maximum spatial resolution that can be achieved.

A more time-consuming approach for reducing these image artifacts is to acquire at least two SSFP images with different RF phase cycling patterns along the RF pulse train (5). This alters the signal intensity and shifts the bands to different locations within the image. Combining these images using maximum intensity projection (MIP) allows one to reduce the appearance of these artifacts. While this combination approach does provide images with diminished artifact, the doubling of acquisition time reduces its appeal, particularly as little increase in signal-to-noise ratio (SNR) is realized in areas of the image not affected by artifact.

Here, we introduce a new implementation of the DESPOT2 T_2 mapping method in which T_2 is determined from a series of phase-cycled SSFP (also termed SSFP-c) images. The method, referred to as phase-cycled DESPOT2, or DESPOT2-c, allows near artifact-free, high-resolution, long TR T_2 mapping without increasing acquisition time. Rather than acquiring two or more sets of multi-angle data, identical except for the phase increment along the RF pulse train, as would be the case for traditional phase-cycled SSFP, we instead divide the full flip angle range into interleaved subsets and acquire each with a different RF phase increment. M_0 and T_2 values are calculated from each subset using a weighted least-squares algorithm (3) and combined using a weighted averaging approach to form final artifact-reduced M_0 and T_2 maps. We show that this method enables us to minimize effects of the SSFP banding artifact in the final parametric maps without requiring additional image acquisition time and provides results superior to those obtained using the traditional SSFP-c approach.

¹Imaging Research Laboratories, Robarts Research Institute, London, Ontario, Canada.

²Department of Medical Biophysics, University of Western Ontario, London, Canada.

³GE Medical Systems, ASL-Central, Waukesha, Wisconsin, USA.

⁴Department of Diagnostic Radiology and Nuclear Medicine, University of Western Ontario, London, Canada.

Grant sponsors: Barnett-Ivey Heart and Stroke Foundation of Ontario (Endowed Chair award to B.K.R.), Canadian Institutes for Health Research; Grant number: MT-11540; GR-14973; Grant sponsors: Canadian Foundation for Innovation, University of Western Ontario, General Electric Medical Systems (Milwaukee, WI).

*Correspondence to: Brian K. Rutt, Imaging Research Laboratories, Robarts Research Institute, P.O. Box 5015, 100 Perth Drive, London, Ontario N6A 5K8, Canada. E-mail: brutt@imaging.robarts.ca

Received 17 December 2003; revised 10 March 2004; accepted 16 March 2004.

DOI 10.1002/mrm.20159

Published online in Wiley InterScience (www.interscience.wiley.com).

© 2004 Wiley-Liss, Inc.

MATERIALS AND METHODS

Phase-Cycled SSFP Theory

Since a thorough theoretical description of SSFP-c is provided in Ref. 5, only a simplified explanation is presented here. It is known that steady state can only be achieved if the precession angle (phase) of the transverse magnetization is the same during all TR intervals. Additionally, the signal measured in an SSFP imaging experiment results from multiple echoes that evolve and combine over several TR intervals. The black bands present in SSFP images occur when the phases of these multiple echoes destructively cancel each other, causing a loss in transverse magnetization, and the longitudinal magnetization becomes saturated. Altering the phase increment along the RF pulse train results in a global shift of the black bands within the image. By acquiring two SSFP images with different RF phase increments, such that the banding artifacts do not overlap, it is possible to reduce the bands by simply combining the two images using maximum intensity projection. Remnants of the bands remain, however, due to the difference in signal intensity between the two images.

Determining T_2 From a Series of Phase-Cycled SSFP Images

To calculate T_2 from a set of variable nutation SSFP image volumes acquired with constant TR and varied α and RF phase increment, the following approach is used. The set of flip angles over which the SSFP image volumes are acquired (SFA) is first divided into two or more subsets (SFA_A, SFA_B, SFA_C, etc), for example, SFA = [10°, 20°, 30°, 40°, 50°, 60°, 70°, 80°] is divided into SFA_A = [10°, 30°, 50°, 70°] and SFA_B = [20°, 40°, 60°, 80°]. Each of these subsets is acquired with a different RF phase increment (for example, 0 and 180°). M_0 and T_2 values are calculated from each subset using the weighted least-squares approach described in Ref. 3 and the appropriate signal equation, yielding parametric maps with parameter inaccuracies in different positions. These individual M_0 and T_2 values are averaged to generate the final, artifact-reduced maps. A weighted average is used to combine the values, where each weight is calculated as the inverse of the sum-of-squares difference between the experimental data and theoretical signal intensities (calculated using the estimated fitted M_0 and T_2 values).

Experimental Validation

To experimentally validate the proposed methodology, phantom and in vivo human brain data were acquired. For the in vivo experiments, informed consent was obtained from the volunteer prior to scanning. All experiments were performed in accordance with ethics approval from the Ethics Review Committee at the University of Western Ontario.

Phantom DESPOT1 and DESPOT2-c data were acquired from an agarose phantom containing eight tubes with varied concentrations of agarose and nickel chloride, providing a 2 × 4 grid of T_1 and T_2 values ($T_1 \approx 250$ ms and 500 ms, $T_2 \approx 30$ ms, 50 ms, 100 ms, and 130 ms). The following sequence parameters were used: DESPOT1: matrix = 256 × 256 × 128, field of view (FOV) = 18 × 18 ×

9 cm, TR = 7.8 ms, echo time (TE) = 2.4 ms, $\alpha = 3^\circ$ and 12° , bandwidth (BW) = ±15.63 kHz, number of averages (NEX) = 4, and total imaging time for both volumes (T_{scan}) = 8.5 min. DESPOT2-c: matrix = 256 × 256 × 128, FOV = 18 × 18 × 9 cm, TR = 6.4 ms, TE = 3.2 ms, SFA = 10°, 20°, 30°, 40°, 50°, 60°, 70°, and 80° divided into SFA_A = 10°, 30°, 50° and 70°, and SFA_B = 20°, 40°, 60°, and 80°, BW = ±41.67 kHz, NEX = 1, and T_{scan} = 28 min. The RF phase increment, θ , was 0° and 180° for SFA_A and SFA_B, respectively. In addition to these DESPOT2-c data, nonphase-cycled DESPOT2 data were also collected with the same parameters listed (i.e., the RF phase increment was 180° for both SFA_A and SFA_B).

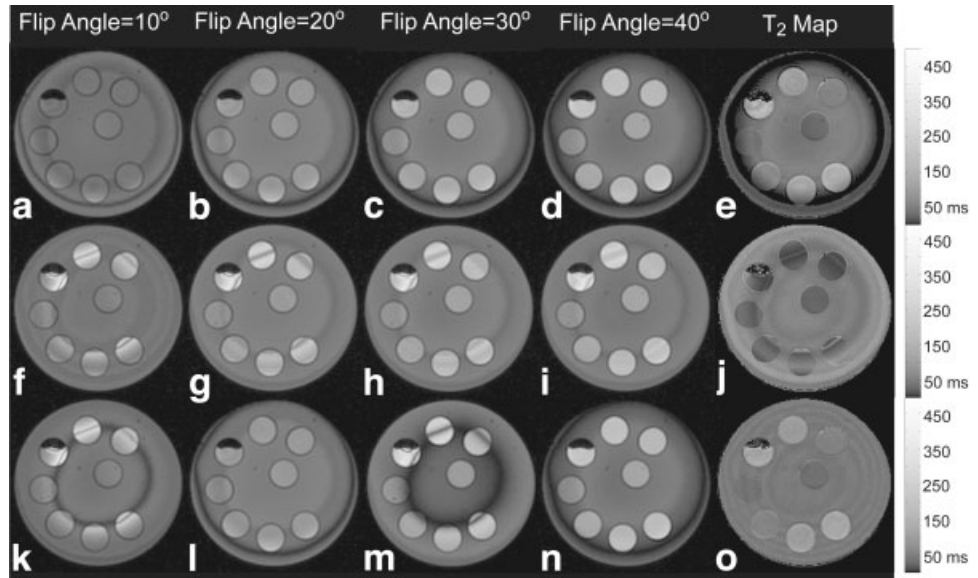
To compare with conventional phase-cycled methodology, DESPOT2 data were acquired using just the SFA_A set of angles. Two sets of data were acquired with the RF phase increment changed from 0° to 180° between the two. Maximum intensity projection was subsequently used to combine the two datasets. Only half of the flip angles were collected in order to maintain a constant exam time between this protocol (referred to as maximum intensity DESPOT2, or, miDESPOT2) and DESPOT2-c. In Ref. 1 we showed that reducing the number of flip angles acquired did not significantly affect the accuracy of the estimated T_2 values.

To evaluate the method in vivo, high-resolution axial brain DESPOT1, DESPOT2-c, nonphase-cycled DESPOT2, and miDESPOT2 data were acquired from a volunteer using the same general parameters listed above with the following flip angles optimized using the approach described in Ref. 3: SFA = 6°, 12°, 17°, 25°, 34°, 43°, 56°, 67°, 77°, and 88° with SFA_A = 6°, 17°, 34°, 56°, and 77°, and SFA_B = 12°, 25°, 43°, 67°, and 88°.

RESULTS

Representative nonphase-cycled DESPOT2 (Fig. 1a–d), maximum intensity projection DESPOT2 (Fig. 1f–i), and DESPOT2-c (Fig. 1k–n) images are shown, along with their corresponding T_2 maps (Fig. 1e,j,m, respectively). Within the nonphase-cycled DESPOT2 parameter map, T_2 voids and areas of artificially low T_2 are seen in the periphery of the phantom. Although the mapping process has removed some of the artifacts within the embedded tubes, the effects are still noticeable, and perhaps accentuated, in the periphery of the phantom. The use of maximum intensity projection to combine images acquired at each flip angle using different RF phases does remove the T_2 voids from the calculated map; however, remnants of the banding artifacts are still present throughout the map and the T_2 values within each tube has clearly been corrupted, with the T_2 values being almost constant between the eight tubes. In reality, the T_2 values of the tubes are not the same but range from ~30 ms to ~130 ms. Using our proposed DESPOT2-c method, the influence of the banding artifacts on the T_2 map is significantly reduced and is only slightly noticeable in the surrounding agarose. Within the nickel chloride-doped tubes, the effects of the banding artifacts are almost completely removed. T_2 values (±SD) calculated for each tube (starting in the center and spiraling outwards counterclockwise) were: 33 (2) ms, 51 (4) ms, 87 (9) ms, 121 (13) ms, 27 (5) ms, 48 (9) ms, 98 (11) ms, and

FIG. 1. Representative phantom images and T_2 maps calculated using non phase-cycled DESPOT2 method (images shown in **a–d** and resulting T_2 map shown in **e**), DESPOT2 data acquired with phase cycling and combined using maximum intensity projection before T_2 calculation (images shown in **f–i** and T_2 map shown in **j**) and our proposed DESPOT2-c approach (images shown in **k–n** and T_2 map shown in **o**). Exam time was held constant in all three protocols.



117 (14) ms, which agree well with gold standard values calculating using a multiecho spin-echo approach (32 ms, 51 ms, 88 ms, 130 ms, 33 ms, 53 ms, 92 ms, and 125 ms). These results show the method to have good accuracy and precision with an average agreement between DESPOT2-c and spin-echo values of 6.4% and an average T_2 -to-noise ratio (average T_2 divided by the SD) of 9.8.

High-resolution T_2 maps of the brain calculated from the nonphase-cycled DESPOT2, miDESPOT2, and DESPOT2-c data are shown in Fig. 2a–c, respectively. Within the nonphase-cycled T_2 map, voids or hypointensities are clearly present in the frontal lobe region and extend back almost to the thalamic and deep-brain regions. These artifacts ostensibly limit the utility of the DESPOT2 approach for detailed, accurate comparisons of T_2 in neuropathology. While this artifact is significantly reduced in the miDESPOT2 map, mild hypointensities remain throughout the frontal lobe region and right side of the brain (seen on the left side of the image). The artifacts are completely removed within the DESPOT2-c T_2 map, demonstrating the in vivo utility of the method. Average T_2 values (and SDs) calculated from regions of interest placed within common brain tissues were: frontal white matter = 64 (8) ms, frontal gray matter = 101 (17) ms, caudate nucleus = 86 (9) ms, thalamus = 73 (7) ms, and cerebral spinal fluid = 1870 (144) ms. These values agree well with those presented previously (6) using conventional T_2 mapping methods and verify that the averaging process does not significantly degrade the accuracy of the T_2 estimates. These results also show the high accuracy and precision of the method in ultra-high-resolution (0.34 mm^3 voxels) maps.

DISCUSSION

The combination of the DESPOT1 and DESPOT2 T_1 and T_2 mapping methods has introduced the possibility of performing ultra-high-resolution ($<0.34 \text{ mm}^3$ isotropic resolution) T_1 and T_2 mapping in vivo. The ability to achieve such high and isotropic spatial resolution should provide

new opportunities for the detailed investigation of T_1 and T_2 changes in neurological disorders. However, the conventional DESPOT2 method is limited by the T_2 inaccuracies that occur in regions of field inhomogeneity, resulting from the SSFP banding artifact. In this work, we presented an alternative implementation of DESPOT2 incorporating RF phase-cycling in order to reduce the effect of these bands. To avoid increases in exam time, the complete range of flip angles (normally used in DESPOT2) is divided into subsets, each of which is acquired with a different RF phase increment. T_2 maps are calculated from each of these subsets and then combined using a weighted averaging technique to generate the artifact-suppressed map. A further benefit of this approach is that, unlike maximum intensity projection, which affords no increase in image SNR despite the increase in image acquisition time, areas that are free of artifact in all subset maps realize some increase in SNR as a result of the averaging of data.

Traditionally, SSFP-c is performed by acquiring the same image volume with two different RF phase increments (yielding I_A and I_B) followed by a maximum intensity projection to combine the two volumes (I_C). While this methodology provides anatomical images with the banding artifacts significantly reduced, it fails when directly applied in conjunction with DESPOT2. This failure is a result of the signal modulation that occurs as a result of the RF phase increment. When the MIP algorithm is applied to the set of images acquired at each flip angle (I_A and I_B), the signal intensity value assigned to a specific voxel in the resulting image, I_C , may come from either I_A or I_B and may not be the same for all flip angles. This effect is more pronounced at low flip angles (i.e., $<30^\circ$), as illustrated by the middle row in Fig. 1 and demonstrated graphically in Fig. 3, where we show the spectral response of the SSFP sequence using no RF phase increment, an increment of 180° , and the MIP of the two spectral responses. Clearly, at high flip angles the MIP signal intensity is adequately approximated by a flat line across all frequencies; however, at low flip angles considerable signal variation across the spectrum still exists. As a result of this effect, a mixture

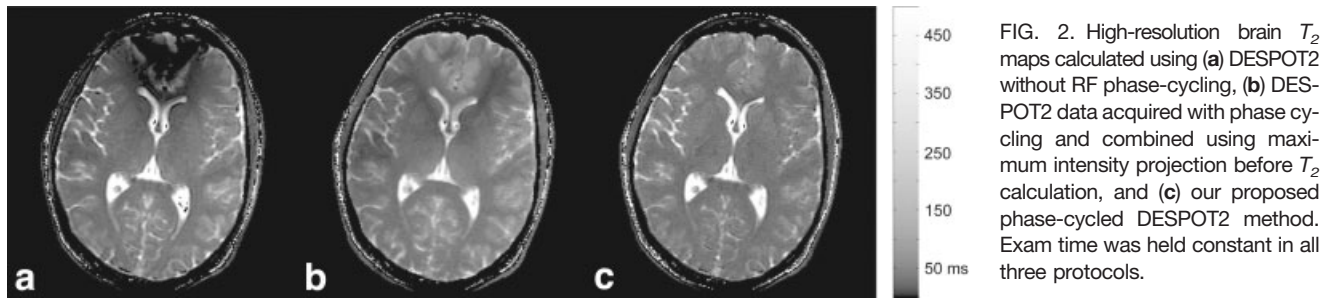


FIG. 2. High-resolution brain T_2 maps calculated using (a) DESPOT2 without RF phase-cycling, (b) DESPOT2 data acquired with phase cycling and combined using maximum intensity projection before T_2 calculation, and (c) our proposed phase-cycled DESPOT2 method. Exam time was held constant in all three protocols.

of values from I_A and I_B will occur along the signal intensity vs. flip angle curve, yielding corrupted T_2 values. A possible solution to this is to calculate T_2 maps from the I_A and I_B image sets first and then combine the maps rather than the raw signals prior to T_2 calculation. This is essentially the approach taken in DESPOT2-c, in which a weighted-average approach was found to be the best T_2 combination method.

The DESPOT2-c method offers the best trade-off between exam time and artifact reduction. Although T_2 corruption is still present around the periphery of the bands, it is significantly improved compared with the MIP implementation. This corruption is due to artificially low T_2 values calculated from one or more of the angle subsets being included in the weighted average. To minimize this effect, an additional filtering or thresholding step could be added in which T_2 values with weights lower than some value are excluded.

An additional variable in the DESPOT2-c method is the number of angle subsets used. In the work presented here, only two subsets (and two RF phases) were used. It is reasonable to assume that further subdividing the complete angle range may result in additional reductions in artifact, as more T_2 values would be included into the

weighted average, reducing the influence of corrupted values. However, as has been previously noted in Refs. 1 and 3, flip angle choice dramatically influences T_2 estimate precision. Thus, care must be taken in choosing the flip angles acquired with each RF phase.

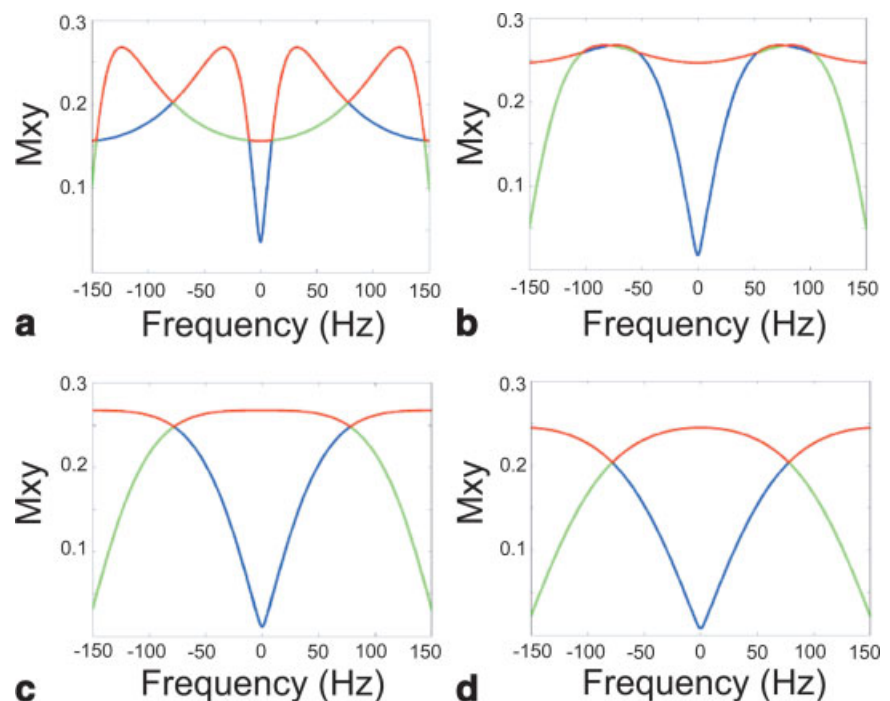
CONCLUSION

A primary limitation of the DESPOT2 T_2 mapping method has been the restriction in spatial resolution imposed by TR considerations. Or alternatively, the limited T_2 accuracy that occurs in regions of field inhomogeneity resulting from long TR, which is especially problematic for high spatial resolution scans. Here we have presented a novel implementation of DESPOT2 incorporating RF phase-cycling which permits correction for the SSFP banding artifacts without requiring additional increases in acquisition time. The method permits near artifact-free, ultra-high-resolution T_2 mapping in a clinically feasible time.

ACKNOWLEDGMENT

We thank Jason A. Polzin (GE Medical Systems) for assistance in pulse sequence development.

FIG. 3. SSFP frequency response curves for an SSFP experiment with no phase increment (blue curve), with a phase increment of 180° (green curve), and the maximum intensity projection of the two (red curve) for a species with $T_1 = 500$ ms, $T_2 = 65$ ms, TR = 6.4 ms, and flip angles (a) 20° , (b) 40° , (c) 60° , and (d) 80° . Resonance offset values range from $-1/TR$ to $1/TR$.



REFERENCES

1. Deoni SCL, Rutt BK, Peters TM. Rapid combined T_1 and T_2 mapping using gradient recalled acquisition in the steady-state. *Magn Reson Med* 2003;49:515–526.
2. Christensen KA, Grand DM, Schulman EM, Walling C. Optimal determination of relaxation times of Fourier transform nuclear magnetic resonance. Determination of spin-lattice relaxation times in chemically polarized species. *J Phys Chem* 1974;78:1971–1977.
3. Deoni SCL, Peters TM, Rutt BK. Determination of optimal angles for variable nutation proton magnetic spin-lattice, T_1 , and spin-spin, T_2 , relaxation times measurement. *Magn Reson Med* 2004;51:194:199.
4. Hargreaves BA, Vasanawala SS, Pauly JM, Nishimura DG. Characterization and reduction of the transient response in steady-state MR imaging. *Magn Reson Med* 2001;46:149–158.
5. Zur Y, Wood ML, Neuringer LJ. Motion-insensitive, steady-state free precession imaging. *Magn Reson Med* 1990;16:444–459.
6. Breger RK, Rimm AA, Fisher ME, Papke RA, Haughton VM. T_1 and T_2 measurements on a 1.5T commercial MR imager. *Radiology* 1989;171:282–276.